GLO22759

Economic Geology
Vol. 79, 1984, pp. 759–767

HYDROTHERMAL ALTERATION ZONING IN THE BEOWAVE GEOTHERMAL SYSTEM, EUREKA AND LANDER COUNTIES, NEVADA

DAVID R. COLE* AND LARISSA I. RAVINSKY

Earth Science Laboratory, University of Utah Research Institute, Salt Lake City, Utah 84108

Introduction

The Beowawe geothermal system, also known as the Geysers, lies 30 km (18.6 mi) southeast of Battle Mountain, astride the Lander-Eureka county line in the Whirlwind Valley of north-central Nevada (Fig. 1). Beowawe ranks among the hottest of the numerous known liquid-dominated systems in the Great Basin (Garside and Schilling, 1978). The system is marked by the presence of hot springs and fumaroles associated with a large opaline sinter terrace. The terrace has developed along the fault-controlled Malpais rim which bounds the southeast margin of Whirlwind Valley.

Presently most of the hot water production is from uncapped exploration wells and numerous springs. The estimated combined discharge is about 400 l per min (Renner et al., 1975). The temperature of the boiling springs is around 95°C, which is the boiling point of water at the 1,524-m elevation of the sinter terrace. Downhole temperature measurements and chemical geothermometers show subsurface temperatures of 200° to 250°C with an average temperature of about 230°C being most probable. At depths greater than about 25 m, the measured temperatures are significantly less than the temperatures predicted for the boiling of pure water. The geothermal waters are dilute, slightly alkaline, sodium-bicarbonate-sulfate solutions (see Nolan and Anderson, 1934; and Table 1).

Drill cuttings are available for study from three deep (>1,500 m) geothermal exploration wells: Ginn 1-13 (2,915 m), Rossi 21-19 (1,733 m), and 85-18 (1,807 m). These drill cuttings were systematically studied by petrographic (125 thin sections) and X-ray diffraction (more than 175 X-ray diffractograms) techniques. Petrographic studies of alteration mineralogy of the drill cuttings were limited by the small chip size (averaging less than 1 cm) which prohibited the accurate determination of paragenetic relationships. In this paper, alteration mineralogy from the various wells is described, and alteration patterns and metal zoning characteristic of the reservoir rocks are defined.

Geologic Setting

Struhsacker (1980) gives the most thorough description of the stratigraphic and structural framework of the Beowawe area. Other recent geologic summaries are given by Zoback (1979) and Garside and Schilling (1979). Figure 1 is a generalized geologic map of the study area showing the locations of the three deep wells. Figures 2 through 4 give more detailed stratigraphic information for these wells.

The Beowawe geothermal system lies along the Malpais fault zone at the base of the Malpais rim. Major fault systems active from pre-Tertiary to the present have controlled the deposition of volcanic rocks, the topography, and, apparently, the present geothermal fluid flow. Rocks exposed within the geothermal area include siliceous Ordovician eugeosynclinal rocks, Tertiary volcanic rocks ranging from basalt to dacite, and Tertiary and Quaternary gravels.

Tertiary lava flows and tuffaceous sediments crop out on the Malpais dip slope. The Malpais scarp exposes an older normal fault system, the Dunphy Pass fault zone, that has a northwest trend. This Oligocene to Miocene fault zone forms the eastern margin of a major northwest-trending graben that is part of the southern extension of a 750-km-long linear aeromagnetic and structural feature called the Oregon-Nevada lineament (Stewart et al., 1975). The Tertiary volcanic section within the graben is approximately 1,400 m thick; east of the Dunphy Pass fault zone it is only 100 m thick. The underlying Ordovician Valmy Formation is a severely fractured sequence of siliceous eugeosynclinal sediments that are part of the Roberts Mountains thrust sheet. Carbonaceous siltstone, chert, and quartzite of the Valmy Formation crop out along the Malpais rim east of the Dunphy Pass fault zone and are encountered by the deep geothermal test wells in Whirlwind Valley. Tertiary diabase dikes that intrude both the Valmy and the volcanic rocks are thought to be the source for the pronounced aeromagnetic anomaly associated with the Oregon-Nevada lineament and the feeders for the Tertiary volcanic sequence filling the graben (Robinson, 1970).

Hydrothermal Alteration

The types and distribution of secondary minerals are shown, together with simplified geologic sections and thermal profiles through the deep drill holes in Figures 2 through 4. As in other geothermal systems (Browne, 1978), temperature, rock type, and the pattern of fluid circulation are the three main factors controlling the style and intensity of alteration in this area. Hypogene alteration at depth has converted primary plagioclase into a variety of hydrothermal

* Present address: Chemistry Division, Oak Ridge National Laboratory, Oak Ridge, Tennessee 37830.

0361-0128/84/309/759-9$2.50

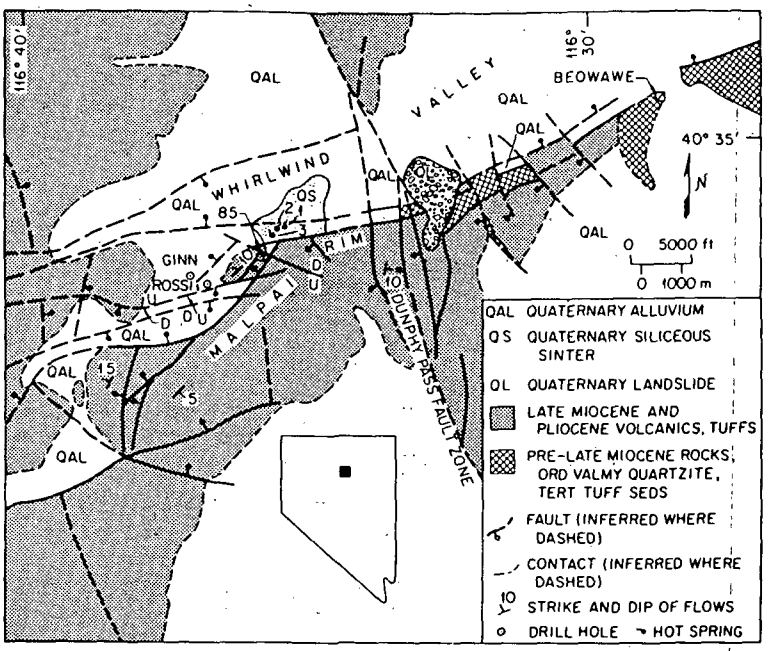

FIG. 1. Generalized geologic map of the Beowawe area (modified from Struhsacker, 1980).

minerals including zeolites, kaolinite, smectite, illite, chlorite, calcite, quartz, and epidote. The ferromagnesian minerals are altered to chlorite, illite, smectite, quartz, calcite, epidote, and pyrite. The fine-grain groundmass is typically altered to quartz, calcite, smectite, assorted zeolites, and chlorite. Supergene

TABLE 1. The Chemical Composition of Fluids from the Beowawe Area

	(1) Hot spring	(2) Hot spring	(3) Hot spring	(4) Well	(5) Well	(6) Well
T°C	89	89	95	160	211	198
T°C (7)	192	186	203	240	218	238
pH (8)	8.6	8.4	8.5	9.1	8.4	8.1
Na (ppm)	219	206	204	277	203	143
K (ppm)	18	14	24	35	30	14
Ca (ppm)	12	1	1	2.5	11	24
Mg (ppm)	1	0.5	0.5	0.3	0.3	7.1
Li (ppm)	1.5	1.4	1.5	1.9	1.4	0.9
B (ppm)	2.0	1.8	1.9	2.0	1.7	0.9
SiO_2 (ppm)	236	218	274	436	335	427
HCO_3 (ppm)	345	340	159	175	247	143
CO_3 (ppm)			196	92	12.5	1.6
SO_4 (ppm)	99	92	107	76	47	27.7
Cl (ppm)	31	19	36	67	59	25
F (ppm)	18	22	15	12.2	7.9	2.8

(1) Hot spring sampled 12-3-81, location 1 in Figure 1
(2) Hot spring sampled 12-3-81, location 2 in Figure 1
(3) Boiling hot spring sampled 12-3-81, location 3 in Figure 1
(4) Chevron well 85-18, analyses given by Iovenitti (1981); see Figure 1 for location. Well depth is 1,804 m (5,920 ft). Sample taken at well head (average gas pressures and compositions from Vulcan Wells 2 and 3 used to correct for CO_2 loss, etc.; see Cosner and Apps, 1978, for data). pH (determined in laboratory) is high because of CO_2 loss
(5) Chevron well Ginn 1-13, analyses from open-file data release, Earth Science Laboratory. See Figure 1 for location. Well depth is 2,915 m (9,563 ft). Gas pressures and compositions estimated in similar manner as well 85-18 (see note 4)
(6) Chevron well Rossi 21-19, analyses from open-file data release, Earth Sci. Lab. See Figure 1 for location. Well depth is 1,733 m (5,686 ft.). Gas pressures and compositions estimated in similar manner as well 85-18 (see note 4)
(7) Temperature calculated from the silica geothermometer (Fournier and Rowe, 1966)
(8) pH of hot springs measured at temperature of spring; well water pH measured at about 20°C in the laboratory

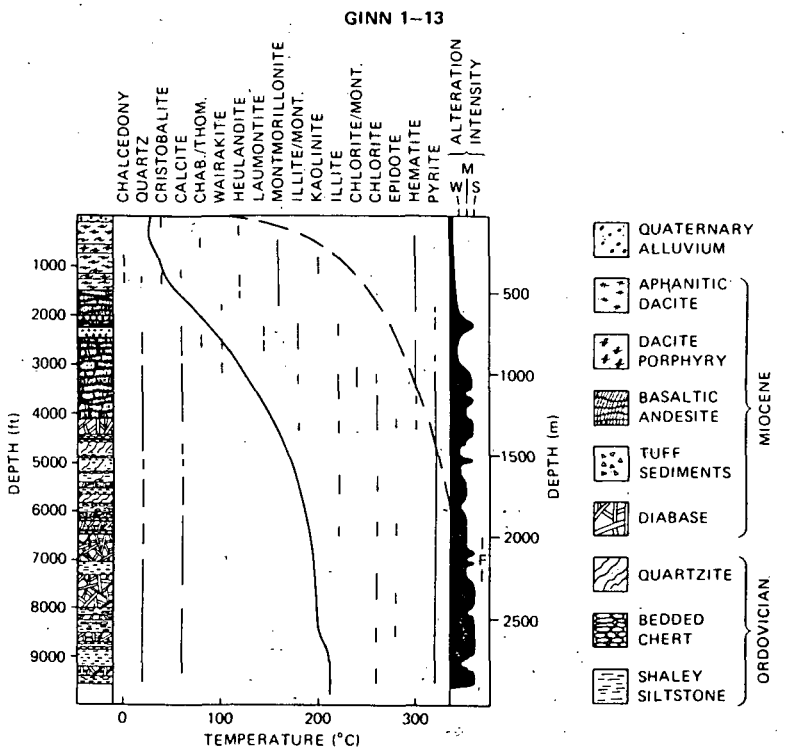

FIG. 2. Distribution of alteration minerals in drill hole Ginn 1-13. Left column shows a generalized stratigraphic section of rock units penetrated by drill hole; lithologic boundaries marked with horizontal lines. Vertical lines indicate the distribution of identified phases. The measured thermal profile is given by the solid curve; reference boiling temperature for pure water is given by the dashed curve. The alteration intensity is described as weak (W), moderate (M), or strong (S). Abbreviations: chab = chabazite, thom = thomsonite, mont = montmorillonite, and F = fracture zone.

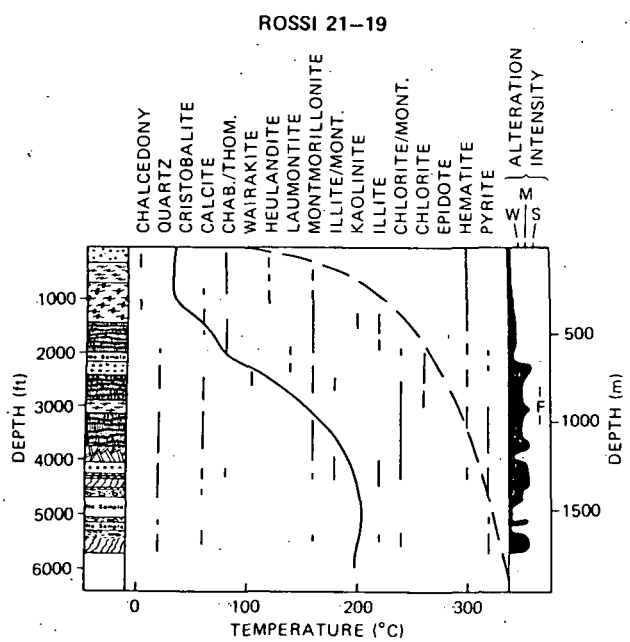

FIG. 3. Distribution of alteration minerals in drill hole Rossi 21-19. Refer to Figure 1 for a description of symbols and nomenclature.

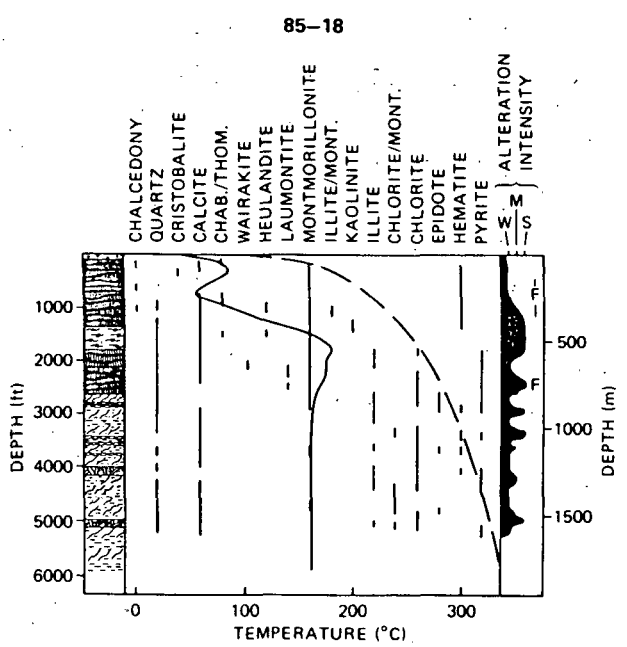

FIG. 4. Distribution of alteration minerals in drill hole 85-18. Refer to Figure 1 for a description of symbols and nomenclature.

alteration associated with the development of the siliceous sinter deposit produced kaolinite, chalcedony, Fe-oxides, and minor alunite.

Silica minerals

The principal silica minerals observed in the Beowawe area are quartz, chalcedony, α-cristobalite, and opal-A. The siliceous sinter deposit is composed predominantly of opal-A with traces of chalcedony and quartz (Rimstidt and Cole, 1983). Chalcedony and α-cristobalite occur in the upper portion of the system at depths less than 450 m, whereas quartz extends to the deepest levels penetrated by the three exploration drill holes. Quartz is by far the most abundant vein mineral observed at depth and occurs with varying amounts of calcite, pyrite, smectites, zeolites, and chlorite. It is common to observe pyrite resorbed by quartz, with both phases, in turn, replacing calcite or clay.

Carbonate minerals

Calcite is found throughout the altered rock in veins and as massive replacement of groundmass and plagioclase phenocrysts. In the volcanic sequence, calcite occurs in veins commonly with quartz and as replacements of lath-shaped plagioclase. Altered Ordovician sediments contain calcite and calcite-quartz veinlets, as well as massive interstitial calcite that has replaced finer grained sedimentary or metasedimentary carbonates.

Zeolite minerals

Zeolites are found in the uppermost part of the drill holes, typically above approximately 900 m. Chabazite is dominant in the cooler (<125°C) and least altered strata but becomes subordinate to thomsonite with increasing depth. The zeolites most commonly found at higher temperatures (125°–175°C) include laumontite, heulandite, and minor amounts of wairakite. Hydrothermal zeolites occur in veinlets accompanying calcite, quartz, or smectite. Additionally, zeolites replace primary plagioclase in the basaltic units and the more sodic feldspars in the dacite. The zeolite zoning with increasing depth and temperature reflects progressive dehydration, where the amount of zeolitic water decreases.

Clay minerals

Clay minerals are the dominant alteration mineral group found in the Beowawe system, with one or more types of clays present at any given depth. The main types of sheet silicates are montmorillonites, illite, chlorite, and mixed-layer minerals of chlorite-montmorillonite. Small amounts of illite appear to be incorporated in some of the mixed-layer mineral structures. The clays occur in veinlets accompanied by quartz, calcite, or pyrite, as well as massive replacements of plagioclase and pyroxene.

Smectite minerals dominate down to approximately 1,000 m depth but are present in minor quantities to greater depths, particularly in the Rossi 21-19 and 85-18 holes (Figs. 3 and 4). Randomly mixed-layer minerals, mainly of smectite-illite and smectite-chlorite are associated with smectites from about 350 to 500 m. Typically, the zone of mixed-layer minerals does not extend below about 1,500 m. Chlorite occurs as the dominant clay from 1,000 m in the Ginn 1-13 hole, whereas in the Rossi 21-19 and 85-18 holes, chlorite dominates below about 700 m. Minor amounts of kaolinite are associated with the dacite or porphyritic dacite flows at depths less than 500 m.

Based on X-ray methods, optical properties, and preliminary electron microprobe analyses, the smectites are identified as saponites. Saponites associated with the dacites and andesitic basalts are typically iron-magnesium rich with minor quantities of calcium. Hydrothermal saponitic clays found in the diabases and Valmy sediments are more magnesium rich, still with significant concentrations of iron and minor calcium.

Chlorites tend to follow a similar pattern in composition as the saponites. Chlorites formed at the expense of phases in the dacites and basalts are iron-magnesium rich, with insignificant concentrations of calcium. The chlorites associated with the diabases and Valmy sediments are enriched in magnesium relative to chlorites higher in the section.

Epidote

The first appearance of epidote occurs at a depth of about 650 m in hole 85-18 but at a much deeper level in the Ginn 1-13, approximately 1,000 m. Hydrothermal epidote was observed in the Rossi 21-19 hole only at a depth of about 1,700 m. Texturally, epidote occurs either as coarse grains (1.0 mm in long dimension) grown on a quartz substrate in open vugs, in quartz-pyrite veinlets, or as replacements of pyroxene or plagioclase. It is not uncommon to observe calcite replacing epidote occurring in veins.

Oxide-sulfide minerals

Hematite is most common in the uppermost portion of the holes, above approximately 500 m for the Rossi 21-19 and 85-18 holes, and above 1,000 m for Ginn 1-13. Hematite occurs as massive replacements of magnetite, pyroxene, olivine, chlorite, and pyrite, as well as in veins containing various proportions of clay and calcite. The association quartz-hematite was not commonly observed in samples from Beowawe.

Small (<0.25 mm) euhedral cubic pyrite crystals are disseminated throughout much of the groundmass of volcanics at depths greater than about 1,000 m for Ginn 1-13 and Rossi 21-19, and about 600 m in 85-18. Pyrite occurs in association with chlorite, epidote, hematite, and magnetite. Additionally, pyrite

in the dacite and andesitic basalt horizons occurs in veins with quartz or minor calcite. Quartz-pyrite-calcite veins also occur in the diabase but are less common in the Valmy Formation. Pyrite in the volcanics is clearly hydrothermal in origin, whereas some of the pyrite in the Valmy Formation is probably diagenetic or metamorphic.

Alteration Zoning Pattern

Zoning is a characteristic feature of hydrothermal rock alteration at Beowawe and is represented by both clay and nonargillaceous hydrothermal minerals. Based on the detailed mineralogy given in Figures 2 through 4, four zones have been defined exhibiting progressive alteration of the rocks. These zones are summarized in Table 2 and depicted graphically in Figure 5c. For comparison, alteration zoning observed in four other geothermal systems is summarized in Table 2 and shown in Figure 5. These systems are: Broadlands, New Zealand (Fig. 5a) (Browne, 1969, 1971; Browne and Ellis, 1970; Eslinger and Savin, 1973); Otake, Japan (Fig. 5b) (Yamasaki et al., 1970; Hayashi, 1973; Hayashi and Yamasaki, 1976); Roosevelt, Utah (Fig. 5d) (Capuano and Cole, 1982; Ballantyne, 1978; Ballantyne and Parry, 1978; Rohrs and Parry, 1978; Glenn et al., 1981); and Reykjanes, Iceland (Fig. 5d) (Tomasson and Kristmannsdottir, 1972).

At Beowawe, the zoned sequence is characterized by a zeolite zone (I) at the top, followed by a smectite-zeolite zone (II), a smectite (mixed-layer)-chlorite zone (III), and a chlorite-epidote zone (IV) with increasing depth. The alteration appears to be weakly pervasive but with the intensity of alteration increasing markedly within the diabase dikes, the host rock surrounding these dikes, and the major fault zones. This general sequence is approximately duplicated in the other four systems. For example, at Reykjanes, Iceland, Tomasson and Kristmannsdottir (1972) described a zoning sequence of zeolite-smectite, mixed layer clays-prehnite, and chlorite-epidote with increasing depth and temperature. Typically, quartz, calcite, and pyrite are found in varying proportions at most depths in these systems. The Otake system differs significantly only at the top where an acid-alteration cap of alunite plus kaolinite predominates.

Another striking similarity between these five systems, in addition to mineral zoning, is in the geometry of the alteration zones (e.g., Browne, 1978). In all five examples, the boundaries of the various alteration zones closely parallel the configurations of isotherms for the systems. At Beowawe, there is generally an increase in temperature for a given depth as one approaches the sinter deposit, northeast of the three deep holes (see Figs. 1, 5c). The contact between zone II (smectite-zeolite) and zone III (smectite-chlorite) is roughly coincident with the 150°C isotherm. Preliminary inspection of samples from holes drilled through the sinter terrace indicates the presence of clay, chlorite, and minor epidote at depths as shallow as 350 to 400 m where temperatures range from 180° to 205°C.

Because of the complex thermal histories probably represented in these systems, the alteration zones are not always clearly defined and phases predominant in one zone can occur in another. Epidote occurs at

TABLE 2. Summary of Alteration Zones for Five Geothermal Systems[1]

	Beowawe[2]	Broadlands[3]	Otake[4]	Roosevelt[5]	Reykjanes[6]
			A: alunite K: kaolinite		
I	zeol		zeol		
II	mont ± zeol ± chl	mont	mont	mont	mont + zeol
III	mont (mixed-layer) + chl + ep	ill/mont ± ab ± ad	mont + chl (ill/chl) ± ep	ill/mont + chl	ill/mont + chl (prehnite)
IV	chl + ep ± mont (mix-layer)	A: chl + ill/mont + ad B: chl + ill/mont ± ad ± ab		A: chl ± ep B: ep-rich ± chl	A: chl B: ep + chl
V				chl + anhy ± ep	

[1] The numbers (e.g., I, II, III, . . .) and letters given in this table are used in Figure 5

[2] Mineralogic data from this study

[3] Broadlands: data from Browne (1969, 1971), Browne and Ellis (1970), and Eslinger and Savin (1973)

[4] Otake: data from Yamasaki et al. (1970), Hayashi (1973), and Hayashi and Yamasaki (1976)

[5] Roosevelt: data from Capauno and Cole (1982), Ballantyne (1978), Ballantyne and Parry (1978), Rohrs and Parry (1978), and Glenn et al. (1981)

[6] Reykjanes: data from Tomasson and Kristmannsdottir (1972)

Abbreviations: mont = montmorillonite, zeol = zeolite, chl = chlorite, ill = illite, ep = epidote, ab = albite, ad = adularia, anhy = anhydrite

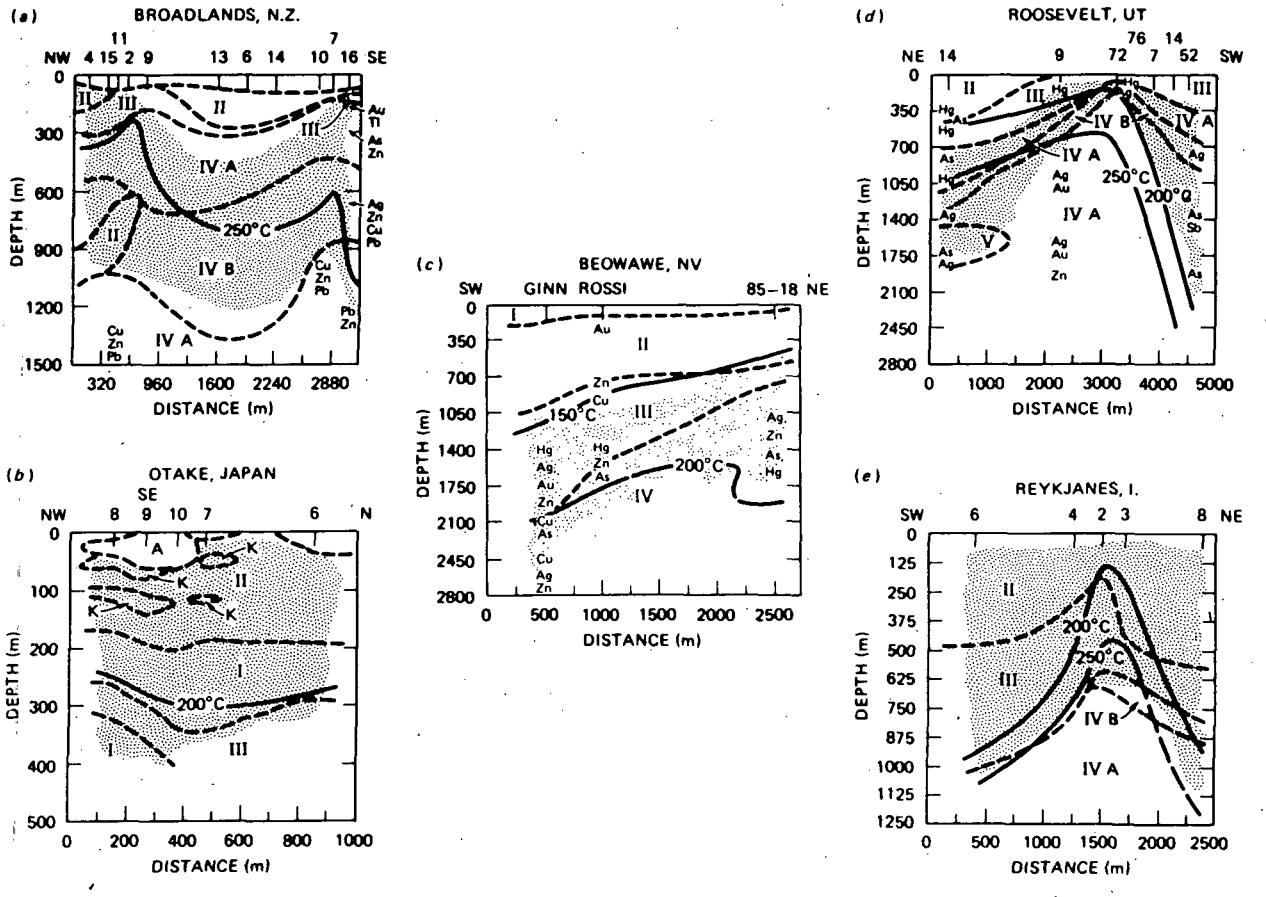

FIG. 5.. Summary of alteration zoning versus depth for five geothermal systems. Drill hole names or numbers are given at the top for each system. The dashed curves represent the approximate boundaries between alteration zones. The numbers and letters correspond to alteration zones described in Table 2. Stippled pattern represents the pyrite distribution. Zones of metal enrichment are indicated by the appropriate chemical symbols (e.g., As = arsenic, Hg = mercury). The distribution of metal enrichments in Broadlands is based on data given by Brown (1971) and Ewers and Keays (1977). Data for Roosevelt are taken from Bamford et al. (1980) and Glenn et al. (1981). For Beowawe (c), metal anomalies in whole rocks are discussed in the text and in Table 3.

several fields (Browne, 1978), usually above 240° to 260°C but in some, such as Reykjanes (Tomasson and Kristmannsdottir, 1972), it apparently occurs down to temperatures less than 100°C. In the Beowawe system, epidote is observed at shallow depths (less than 600 m) and lower temperatures (between 150° and 175°C) in two of the three deep drill holes. Additionally, the high temperature (>220°C) assemblage of illite plus chlorite (Browne, 1978) is present to temperatures less than 150°C at Beowawe.

The temperature-depth-mineral assemblage relationships observed for the Beowawe system suggest that temperatures have decreased. Also, the abundance of hematite is inconsistent with the relatively reducing conditions that are indicative of the assemblage pyrite plus chlorite. This suggests that the present system is in a state of thermal collapse, with the fluids derived from relatively shallow depths. The high SO_4 in the well discharges supports this contention. Typically, the neutral sodium-bicarbonate-sulfate waters are characteristic of condensates, which would tend to form in the waning system (Mahon et al., 1980). The assemblage zeolite-montmorillonite-hematite is probably associated with this fluid type. The assemblage chlorite-illite-epidote-pyrite, on the other hand, is more indicative of a system where a sodium chloride-type fluid dominates (Rose and Burt, 1979), as is the case for the other geothermal systems described in Table 2 and Figure 5.

Therefore, the mineralogic and textural evidence support a model for Beowawe where a reducing, sodium chloride-type fluid reacted with volcanics and sediments at temperatures probably in excess of 220°C resulting in an assemblage of chlorite-illite-

TABLE 3. Summary of Selected Trace Element Data from the Beowawe, Nevada Geothermal System

Well	Au ppm[1]	Ag ppm[1]	Zn ppm[1]	Cu ppm[1]	Hg ppb[2]	As ppm[3]
Ginn						
$\bar{X}$[4]	0.34	0.79	104.3	33.6	90.2	11.3
σ[5]	1.51	1.89	68.7	31.9	146.2	14.7
n[6]	89	90	90	91	89	89
$>\bar{X} + 2\sigma$[7]	4,800–4,900 ft (6)	5,900–6,000 ft (4) 7,400–7,500 ft (4)	5,400–5,500 ft (248) 9,000–9,100 ft (309)	7,400–7,500 ft (101)	4,200–4,300 ft (500)	
$>\bar{X} + 3\sigma$[8]	5,600–5,700 ft (7) 6,100–6,200 ft (10)	5,600–5,700 ft (9) 5,700–5,800 ft (8) 9,100–9,200 ft (11)	5,200–5,300 ft (361) 9,100–9,200 ft (481)	6,300–6,400 ft (251) 9,100–9,200 ft (150)	4,300–4,400 ft (1,200)	6,300–6,400 ft (60) 7,000–7,100 ft (80) 7,100–7,200 ft (90)
Rossi						
$\bar{X}$	0.68		114.1	37.1	81.5	12.7
σ	1.80		54.2	57.0	101.4	19.4
n	55		55	50	52	51
$>\bar{X} + 2\sigma$	100–200 ft (5) 400–500 ft (5) 1,500–1,600 ft (5) 1,600–1,700 ft (6)				4,400–4,500 ft (310)	
$>\bar{X} + 3\sigma$	0–100 ft (7)		3,000–3,100 ft (337) 5,600–5,700 ft (346)	3,000–3,100 ft (395)	4,600–4,700 ft (409) 5,300–5,400 ft (420)	5,500–5,600 ft (90) 5,600–5,700 ft (100)
85-18						
$\bar{X}$		1.33	117.5	41.2	125.7	24.6
σ		4.94	54.3	28.7	107.9	31.7
n		58	54	51	53	52
$>\bar{X} + 2\sigma$		3,800–3,900 ft (14)	3,500–3,600 ft (236)	3,500–3,600 ft (101) 3,700–3,800 ft (111) 3,800–3,900 ft (107)		4,700–4,800 ft (100) 5,400–5,500 ft (95)
$>\bar{X} + 3\sigma$		4,000–4,100 ft (29) 4,200–4,300 ft (21)	4,300–4,400 ft (370)		4,900–5,000 ft (450)	5,000–5,100 ft (140) 5,100–5,200 ft (120)

[1] The elements Au, Ag, Zn, and Cu were determined by inductively coupled plasma-atomic emission spectroscopy on pulverized (<270 mesh) 100-ft interval whole-rock samples (100-ft interval samples are composites of ten 10-ft interval samples) dissolved by a four-acid digestion procedure (Christensen et al., 1980). The detection limits for these elements are 4, 2, 1, and 1 ppm, respectively. For samples with Au or Ag concentrations below detection, average values for each rock type were taken from Wedepohl (1969). Numbers in parentheses refer to concentrations of metals within a particular depth interval

[2] Hg was determined on pulverized (<270 mesh) 100-ft interval whole-rock samples by the gold film mercury detector. The detection limit is 5 ppb

[3] As was determined on pulverized (<270 mesh) 100-ft interval whole-rock samples by a colorimetric procedure. The detection limit is 1 ppm

[4] $\bar{X}$ = arithmetic mean

[5] σ = standard deviation

[6] n = population size

[7] $>\bar{X} + 2\sigma$: analytical values (in parentheses) are given for depth intervals that exceed a threshold defined as the mean plus two times the standard deviation. Values that exceed this threshold are possibly anomalous

[8] $>\bar{X} + 3\sigma$: analytical values (in parentheses) that exceed this threshold are probably anomalous

epidote-pyrite. As the thermal regime collapsed, this sodium chloride fluid was replaced by a shallow, oxidized sodium-bicarbonate-sulfate water which reacted with the host rocks at temperatures less than about 200°C, producing the alteration assemblage montmorillonite-zeolite-hematite-carbonate.

Metal Zoning

In addition to the alteration zoning, mobile trace elements (e.g., Au, Ag, As, Hg, Sb, Cu, Pb, Zn) form characteristic hypogene dispersion patterns in many geothermal systems (e.g., Browne, 1969, 1971; Ewers and Keays, 1977; Weissberg, 1969; White, 1981). Because of the mineralogical and geochemical similarities between geothermal systems and many epithermal ore deposits, the relationship between alteration zoning and metal enrichments in active geothermal systems may provide some insight into the behavior of metals in epithermal environments (e.g., White, 1955, 1981; Wetlaufer et al., 1979).

A summary of selected trace element data (Au, Ag, Zn, Cu, Hg, As) for the Beowawe system is given in Table 3. In addition to the mean ($\bar{X}$) and standard deviation (σ) of each element for the total sample population, anomalous values and their depths are given based on two models, $\bar{X} + 2\sigma$ and $\bar{X} + 3\sigma$. Zones of anomalous metal enrichment at Beowawe based on the latter model are indicated in Figure 5c, along with metal enrichments for selected wells from Broadlands (Fig. 5a) and Roosevelt (Fig. 5d).

A comparison of the data from Table 3 with the drill hole stratigraphy given in Figures 2 through 4 indicates that of the 46 anomalies (based on both models), approximately 57 percent are associated with diabase dikes (within the dike or ±200 ft of the dike). Ag, Zn, and Cu are strongly affiliated with dikes, where 88, 75, and 71 percent of the anomalies determined for these elements, respectively, are located within or near dikes (±200 ft). There also appears to be a zoning pattern related to the levels of the dike emplacement. For example, in the Ginn well, the upper two major dike zones are enriched in all metals described in Table 3 (i.e., Au, Ag, Zn, Cu, Hg, As), whereas the lower three dike zones (below about 6,000 ft) are enriched in only Cu, As, and Ag. Zn enrichment is observed only in the lowermost dike of this group below about 9,000 ft.

Metal zoning around the dikes is poorly developed except for Cu and Zn. All of the Cu anomalies associated with dikes are located at or near the upper contact of a dike and either Ordovician sediments or Tertiary volcanics. Similarly, five out of the six Zn anomalies associated with diabase dikes are located at the upper contact.

These data suggest that the diabase dikes (mid-Miocene age, ~16.5 m.y.) acted not only as feeders for the overlying basalt and andesite but also were local heat sources responsible for driving fluid convection which produced some of the observed alteration and trace element patterns. Zones of intense chlorite-epidote-pyrite alteration are commonly associated with the diabase dikes, particularly at dike-sediment contacts. It is important to point out that approximately 65 percent of the total number of anomalies are associated with either dikes, lithologic contacts, or fault zones. This implies that fluid flow through the Beowawe system was (and probably still is) restricted to discreet fracture zones or permeable horizons.

The remaining 35 percent of the trace element anomalies (see Table 3) typify a more subtle rock association apparently unrelated to dike emplacement. For example, Au anomalies are associated with dacites and quartz latites high in the stratigraphic section (0–1,200 ft) of well 85-18. Au in the Ginn samples is enriched in the Ordovician sediments at depths near 6,000 ft. In fact, approximately 80 percent of the nondike-related anomalies are located in Ordovician sediments at depths in excess of 4,000 ft.

The Beowawe system exhibits a weak zonation of metals similar to patterns observed at Broadlands (Fig. 5a) and Roosevelt (Fig. 5d). At Beowawe, the lower one-third (6,200–9,300 ft) of the system is characterized by anomalous enrichments in Zn, Cu, Ag, and As, followed by Zn, Au, Ag, and Hg in the next one-third (3,100–6,200 ft), and finally capped by a metal-deficient zone rich only in Au (0–3,100 ft). In Broadlands, the deep base metal zone of Cu-Pb-Zn is overlain by a zone of Ag plus base metals, with an upper zone of Au-As-Tl (Ewers and Keays, 1977). Metal distributions and rock alteration at Broadlands have resulted from rock interaction with a chloride (±bisulfide) fluid at temperatures near 250°C (Weissberg et al., 1979). At Beowawe, an early high-temperature (>220°C?) sodium chloride-rich fluid believed responsible for the reducing alteration assemblage of chlorite-epidote-pyrite probably played a key role in transport and deposition of base and precious metals. As the thermal regime collapsed, this fluid was replaced by a dilute sodium-bicarbonate-sulfate water unable to transport metals. Only the more volatile elements such as Hg continue to move in response to the changes in thermal and fluid flow patterns.

Acknowledgments

This study was supported by the U. S. Department of Energy under contracts DE-AC07-80ID1207 to the Earth Science Laboratory and W-7405-eng-26 to the Union Carbide Corporation (Oak Ridge National Laboratory). Chemical analyses were performed by Ruth Kroneman, Keith Yorgason, Beverly Miller, and Frank Bakke.

August 2, 1983; January 20, 1984

REFERENCES

Ballantyne, G. H., 1978, Hydrothermal alteration at the Roosevelt Hot Springs thermal area, Utah: Characterization of rock types and alteration in Getty Oil Company well Utah State 52-21: Univ. Utah, Dept. Geology Geophysics Topical Rept. 78-1701.a.1.1.4, 23 p.

Ballantyne, J. M., and Parry, W. T., 1978, Hydrothermal alteration at the Roosevelt Hot Springs thermal area, Utah: Petrographic characterization of the alteration at 2 kilometers depth: Univ. Utah, Dept. Geology Geophysics Tech. Rept. 78-1701.a.1.1, 23 p.

Bamford, R. W., Christensen, O. D., and Capuano, R. M., 1980, Multi-element geochemistry of solid materials in geothermal systems and its application. Part I: The hot-water system at the Roosevelt Hot Springs KGRA, Utah: Univ. Utah Research Inst., Earth Sci. Lab. Rept. ESL-30, 168 p.

Browne, P. R. L., 1969, Sulfide mineralization in a Broadlands geothermal drill hole, Taupo volcanic zone, New Zealand: ECON. GEOL., v. 64, p. 156–159.

—— 1971, Mineralization in the Broadlands geothermal field, Taupo volcanic zone, New Zealand: Soc. Mining Geologists Japan, Spec. Issue 2, p. 64–75.

—— 1978, Hydrothermal alteration in active geothermal fields: Ann. Rev. Earth Planet. Sci., v. 6, p. 229–250.

Browne, P. R. L., and Ellis, A. J., 1970, The Ohaki-Broadlands hydrothermal area, New Zealand: Mineralogy and related geochemistry: Am. Jour. Sci., v. 269, p. 97–131.

Capuano, R. M., and Cole, D. R., 1982, Fluid-mineral equilibra in a hydrothermal system, Roosevelt Hot Springs, Utah: Geochim. et Cosmochim. Acta, v. 46, p. 1353–1364.

Christensen, O. D., Kroneman, R. L., and Capuano, R. M., 1980, Multielement analysis of geologic materials by inductively coupled plasma-atomic emission spectroscopy: Univ. Utah Research Inst., Earth Sci. Lab. Rept. 32, 33 p.

Cosner, S. R., and Apps, J. A., 1978, Compilation of data on fluids from geothermal resources in the United States: Univ. California, Lawrence Berkeley Lab. Rept. 5936, 108 p.

Eslinger, E. V., and Savin, S. M., 1973, Mineralogy and oxygen isotope geochemistry of the hydrothermally altered rocks of the Ohaki-Broadlands, New Zealand, geothermal area: Am. Jour. Sci., v. 273, p. 240–267.

Ewers, G. R., and Keays, R. R., 1977, Volatile and precious metal zoning in the Broadlands geothermal field, New Zealand: ECON. GEOL., v. 72, p. 1337–1354.

Fournier, R. O., and Rowe, J. J., 1966, Estimation of underground temperatures from the silica content of water from hot springs and wet-steam wells: Am. Jour. Sci., v. 264, p. 685–697.

Garside, L. J., and Schilling, J. H., 1979, Thermal waters of Nevada: Nevada Bur. Mines Geol., Bull. 91, 163 p.

Glenn, W. E., Hulen, J. B., and Nielson, D. L., 1981, A comprehensive study of LASL C/T-2 Roosevelt Hot Springs KGRA, Utah and applications to geothermal well logging: Los Alamos Scientific Lab. Rept. LA-8686-MS, 175 p.

Hayashi, M., and Yamasaki, T., 1976, Hydrothermal alteration of pyroxene andesites in the Otake geothermal area, Japan: Internat. Symposium on Water-Rock Interaction, Prague 1974, Proc., p. 158–169.

Hayashi, M., 1973, Hydrothermal alteration in the Otake geothermal area, Kyushu: Japan Geothermal Energy Assoc. Jour., v. 10, p. 9–46.

Iovenitti, J., 1981, Beowawe geothermal area evaluation program: Work performed for the Dept. of Energy, contract DE8C08-78ET-27101-1; available from Univ. Utah Research Inst., Earth Sci. Lab., 103 p.

Mohan, W. A. J., Klyen, L. E., and Rhode, M., 1980, Neutral sodium/bicarbonate/sulfate hot waters in geothermal systems: Japan Geothermal Energy Assoc. Jour., v. 17, p. 11–24.

Nolan, T. B., and Anderson, G. H., 1934, The geyser area near Beowawe, Eureka County, Nevada: Am. Jour. Sci., v. 27, p. 215–229.

Renner, J. L., White, D. E., and Williams, D. L., 1975, Hydrothermal convection systems, *in* White, D. E., and Williams, D. L., ed., Assessment of geothermal resources of the United States—1975: U. S. Geol. Survey Circ. 726, p. 5–57.

Rimstidt, J. D., and Cole, D. R., 1983, Geothermal mineralization I: The mechanism of formation of the Beowawe, Nevada, siliceous sinter deposit: Am. Jour. Sci., v. 283, p. 861–875.

Robinson, R. H., 1979, Geothermetric analysis of water samples from Whirlwind Valley, Eureka and Lander Counties, Nevada: Geothermal Resources Council Trans., v. 3, p. 587–590.

Rohrs, D., and Parry, W. T., 1978, Hydrothermal alteration at the Roosevelt Hot Springs thermal area, Utah: Thermal Power Company well Utah State 72-16: Univ. Utah, Dept. Geology Geophysics Topical Rept. 78-1701.a.1.1.3, 23 p.

Rose, A. W., and Burt, D. M., 1979, Hydrothermal alteration, *in* Barnes, H. L., ed., Geochemistry of hydrothermal ore deposits, 2nd ed.: New York, John Wiley and Sons, p. 173–225.

Stewart, J. H., Walkder, G. W., and Kleinhampl, F. I., 1975, Oregon-Nevada lineament: Geology, v. 3, p. 265–268.

Struhsacker, E. M., 1980, The geology of the Beowawe geothermal system, Eureka and Lander counties, Nevada: Univ. Utah Research Inst. Rept. ESL-37, 78 p.

Tomasson, J., and Kristmannsdottir, H., 1972, High temperature alteration minerals and thermal brines, Reykjanes, Iceland: Contr. Mineralogy Petrology, v. 36, p. 123–134.

Wedepohl, K. E., ed., 1969, Handbook of geochemistry: New York, Springer.

Weissberg, B. G., 1969, Gold-silver ore-grade precipitates from New Zealand thermal waters: ECON. GEOL., v. 64, p. 95–108.

Wetlaufer, P. H., Bethke, P. M., Barton, P. B., and Rye, R. O., 1979, The Creede Ag-Pb-Zn-Cu-Au district, Central San Juan Mountains, Colorado: A fossil geothermal system: Nev. Bur. Mines Geol. Rept. 33, p. 159–164.

White, D. E., 1955, Thermal springs and epithermal ore deposits: ECON. GEOL. 50TH ANN. VOL., p. 99–154.

—— 1981, Active geothermal systems and hydrothermal ore deposits: ECON. GEOL. 75TH ANN. VOL., p. 392–423.

Yamasaki, T., Matsumoto, Y., and Hayashi, M., 1970, Geology and hydrothermal alterations of Otake geothermal area, Kujyu Volcano Group, Kyushu, Japan, *in* U. S. Symposium on the Development and Utilization of Geothermal Resources, Pisa, 1970: Geothermics Spec. Issue, v. 2, pt. 1, p. 197–207.

Zoback, M. L., 1979, A geologic and geophysical investigation of the Beowawe geothermal area, north-central Nevada: Stanford Univ. Pub. Geol. Sci., v. 16, 79 p.

Geothermal Resources Council, TRANSACTIONS Vol. 4, September 1980

MODEL FOR A DEEP CONDUIT TO THE BEOWAWE GEOTHERMAL SYSTEM, EUREKA AND LANDER COUNTIES, NEVADA

E. M. Struhsacker and Christian Smith

Earth Science Laboratory Division/Univ. Utah Research Institute
420 Chipeta Way, Suite 120
Salt Lake City, UT 84108

ABSTRACT

A fault set trending N15-35W formed the eastern boundary of a major graben in the Beowawe area in the Late Tertiary. Geologic mapping and dipole-dipole resistivity data suggest that this fault set may have been and continues to be a deep conduit to the Beowawe geothermal system.

INTRODUCTION

The Beowawe Geysers have formed a 850 m long sinter terrace at the base of the Malpais scarp near Battle Mountain, Nevada. They have attracted exploration for geothermal electric power generation. The high-temperature (200+ ^{o}C) hydrothermal system appears to be controlled by the intersection of fault sets that tap deeply circulating water in an area with high regional heat flow (>100 mW $\cdot$ m^{-2}).

DISCUSSION

Aerial photographs reveal a strong north-northwest-trending topographic lineament that transects the Malpais Rim east of White Canyon. We refer to this fracture set as the Dunphy Pass Fault zone (replacing the name Whirlwind-Crescent Fault zone of Smith et al., 1979 to avoid confusion with other similarly named faults in the area). The Malpais scarp slope, immediately east of White Canyon, reveals the juxtaposition of Ordovician Valmy Formation quartzite and siltstone against Tertiary pyroxene dacite flows along north-northwest-trending faults (Figure 1). In White Canyon and on the Malpais dip slope, the N15-35W fault trend forms a horsetail pattern on the map (Plate 1). These faults produced dip-slip motion to the west-southwest. Lithologies encountered in the Ginn and Rossi wells (Chevron, 1979; Smith et al., 1979) and in the Batz well (Zoback, 1979) indicate that as much as 1200 m of Miocene volcanics and younger alluvium accumulated west of the fault zone prior to the growth of the Malpais scarp. Additional northwest-trending faults with small displacements cut the Malpais scarp immediately west and east of White Canyon.

Exposures of veins and alteration reveal that the intersection of the Malpais Fault with the Dunphy Pass Fault zone has been the focus of intense hydrothermal activity. Uplift on the Malpais Fault has exposed a dense swarm of east-west-trending chalcedony-carbonate veins cutting pyroxene dacite at the mouth of White Canyon (Figure 2). Several large, near-vertical veins of one to two m thick stand in relief over a 0.6 km strike length. Adjacent fault breccia, gouge, and country rock are pervasively argillized or silicified. The major veins are not traceable to the east of the north-northwest-trending fault contact between the dacite and the Valmy quartzites and siltstones. However, abundant chalcedony veinlets and veins with thicknesses up to 0.3 m continue eastward through the highly fractured Valmy to the young landslide. The abundance of chalcedony veins drops drastically in Valmy exposures to the east of the landslide. The exposed vein swarm and attendant zone of alteration extends 0.2 km south of the mouth of White Canyon. A linear zone of chalcedony and opal-filled fractures and open spaces in a paleo-colluvium or dacite flow breccia unit on the eastern wall of White Canyon continues southward from the vein swarm for one km up the canyon. Several thin chalcedony veins strike N70E, and cross this zone in the middle of the White Canyon gorge. These veins appear to follow fractures subsidiary to the main Malpais Fault. The Malpais Fault truncates the veins to the west at the edge of Whirlwind Valley.

The elevation of the top of the alteration zone increases in a steplike manner eastward along the Malpais scarp slope on the west side of the landslide detachment zone. The observed displacements of the alteration zone indicate renewal of motion on the Dunphy Pass Fault zone subsequent to the deposition of the chalcedony veins. The Dunphy Pass Fault zone may, therefore, be permeable at depth.

The alteration features appear to decrease in age westward from this fault intersection to the active sinter terrace. Sealing of the shallow portions of the conduit may have diverted hydrothermal fluids to the west along the Malpais Fault zone, ultimately producing the sinter terrace above permeable fault intersections.

Numerical modeling of 2000 ft. dipole-dipole resistivity data taken along north-south lines in

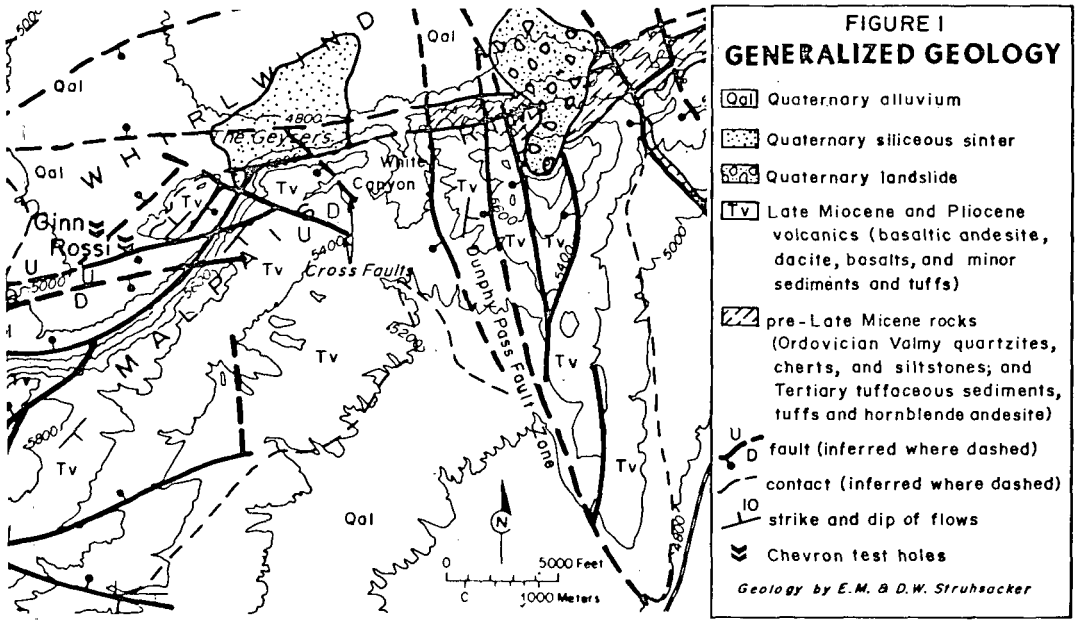
FIGURE 1
GENERALIZED GEOLOGY
Qal Quaternary alluvium
Quaternary siliceous sinter
Qls Quaternary landslide
Tv Late Miocene and Pliocene volcanics (basaltic andesite, dacite, basalts, and minor sediments and tuffs)
pre-Late Micene rocks (Ordovician Valmy quartzites, cherts, and siltstones; and Tertiary tuffaceous sediments, tuffs and hornblende andesite)
U D fault (inferred where dashed)
contact (inferred where dashed)
10 strike and dip of flows
Chevron test holes
Geology by E.M. & D.W. Struhsacker
Qal
Tv
Ginn
Rossi
White Canyon
Cross Faults
Dunphy Pass Fault Zone
5000 Feet
1000 Meters

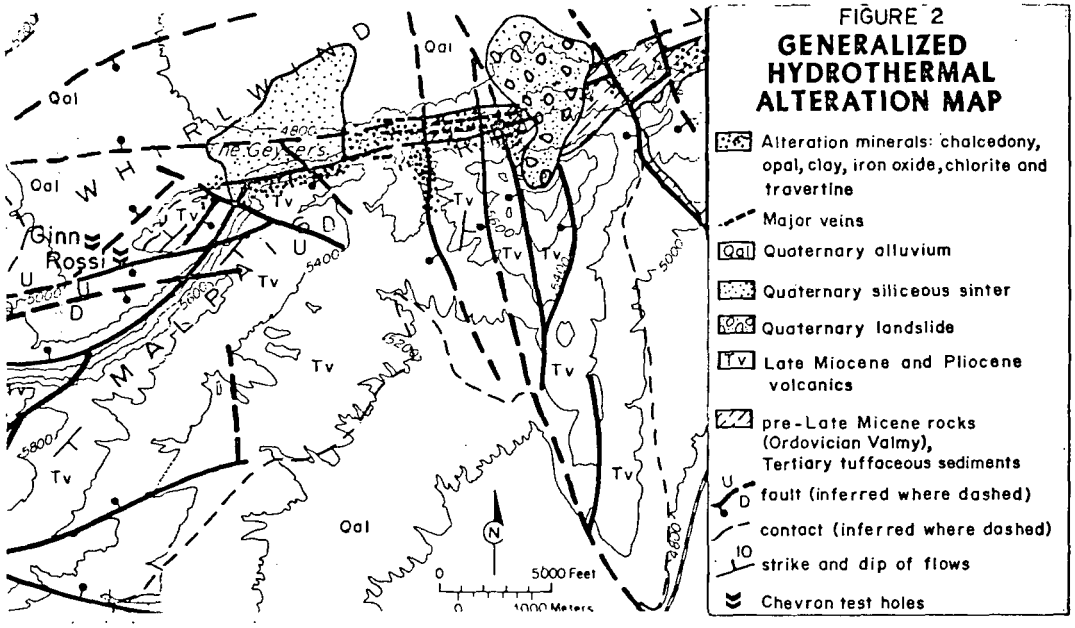
FIGURE 2
GENERALIZED HYDROTHERMAL ALTERATION MAP
Alteration minerals: chalcedony, opal, clay, iron oxide, chlorite and travertine
Major veins
Qal Quaternary alluvium
Quaternary siliceous sinter
Qls Quaternary landslide
Tv Late Miocene and Pliocene volcanics
pre-Late Micene rocks (Ordovician Valmy), Tertiary tuffaceous sediments
U D fault (inferred where dashed)
contact (inferred where dashed)
10 strike and dip of flows
Chevron test holes
Qal
Tv
Ginn
Rossi
5000 Feet
1000 Meters

July, 1974 (Smith, 1979) suggest a 5 ohm-m low-resistivity zone below a depth of 915 m at the intersection of the Malpais and Dunphy Pass Fault zones. This zone extends to the west and crops out at the sinter terrace. These data do not distinguish whether this and other low-resistivity zones indicate hydrothermally altered rock or active conduits for hot water. However, just east of White Canyon, a 300 ohm-m body above the low-resistivity anomaly may reveal a silicified cap of Ordovician and Tertiary rocks above a deep conduit.

The intense hydrothermal activity on the sinter terrace, at the structural intersections of the Malpais Fault zone and the two cross faults indicates that fracture conduits within the Malpais Fault zone lie beneath the sinter terrace. East-west fractures passing through and north of the sinter terrace are probable conduits feeding hot springs on the flats at the foot of the terrace. Small deposits of old sinter along the South Cross Fault (Oesterling, 1962) at the top and base of the Malpais scarp indicate former shallow permeability on this cross fault. However, the traces of the cross faults are obscure and surficial evidence of hydrothermal activity are lacking on the Malpais dip slope to the south.

Models of the north-south dipole-dipole data reveal an anomalous low-resistivity zone that extends below the Malpais Rim southeast of The Geysers (Figure 4). However, the southern margin and lateral extent of the anomaly can not be resolved. To define better the resistivity distribution of the Malpais Rim, data were taken along three additional dipole-dipole lines oriented perpendicular to the Dunphy Pass Fault zone in April, 1980. Numerical modeling of these data incorporate the complex effects due to topography and confirm and refine the location of the low resistivity zone. Figure 4 shows the interpreted intrinsic resistivity at 915 m elevation, 550-800 m depth.

Resistivities less than 30 ohm-m follow a straight and narrow zone that trends southeast of The Geysers. This linear anomaly cuts the Malpais Rim for a distance of at least 4250 m and is rarely wider than 900 m. The lowest interpreted resistivity (10 ohm-m) occurs not at The Geysers where they might be expected but 1200-1800 m to the southeast on the west flank of White Canyon. Conduction by clay minerals produced during episodes of hydrothermal activity prior to the establishment of the present system may be the sole cause of the resistivity anomaly. However, the anomaly lies between the southeastward projection of the cross - faults that bound the area of modern surficial hydrothermal activity. If hot water within or between the faults causes the resistivity anomaly, there may be hot water below the dip slope of the Malpais Rim along segments of the Dunphy Pass Fault zone. Possible aquifers include fractured or jointed volcanic rocks or quartzite.

CONCLUSIONS

We have identified two structurally controlled zones that may link the Beowawe Geysers to a major north-northwest-trending fault zone. Thermal gradient holes to be drilled in the summer of 1980 will test both suggested links. The Dunphy Pass fault zone is the deepest structure crossing the Malpais Rim. Its intersection with the Malpais fault zone is therefore the most likely structure in the Beowawe area to accomodate deep conduits to the hydrothermal system.

ACKNOWLEDGEMENTS

This research was supported under the Industry Coupled Program of the Department of Energy, Division of Geothermal Energy, Contract No. DE-AC07-80ID12079.

REFERENCES

Chevron Resources Co., 1979, Open-File data on Beowawe released by Earth Science Laboratory, Salt Lake City, Utah.

Oesterling, W. A., 1962, Geothermal power potential of northern Nevada: Text of paper presented at the 1962 Pacific Southwest Mineral Industry Conference of the A.I.M.E.

Smith, Christian, Struhsacker, E. M., and Struhsacker, D. W., 1979, Structural inferences from geologic and geophysical data at the Beowawe KGRA, North-central Nevada: Geothermal Resources Council Trans. Vol. 3, p. 659-662.

Zoback, M. L., 1979, Geologic and geophysical investigation of the Beowawe geothermal area, north-central Nevada: Stanford University School of Earth Sciences - Geological Sciences Series, v. XVI.